Hindawi
Journal of Control Science and Engineering
Volume 2019, Article ID 8146901, 17 pages
https://doi.org/10.1155/2019/8146901

*Research Article*

# Nonsingular Fast Terminal Sliding Mode Tracking Control for a Class of Uncertain Nonlinear Systems

**Siyi Chen, Wei Liu, and Huixian Huang**

*College of Information Engineering, Xiangtan University, Xiangtan 411105, China*

Correspondence should be addressed to Wei Liu; 601312957@qq.com

Received 19 January 2019; Revised 18 April 2019; Accepted 30 April 2019; Published 30 May 2019

Academic Editor: Radek Matušů



Aiming at the tracking control problem of a class of uncertain nonlinear systems, a nonsingular fast terminal sliding mode control scheme combining RBF network and disturbance observer is proposed. The sliding mode controller is designed by using nonsingular fast terminal sliding mode and second power reaching law to solve the problem of singularity and slow convergence in traditional terminal sliding mode control. By using the universal approximation of RBF network, the unknown nonlinear function of the system is approximated, and the disturbance observer is designed by using the hyperbolic tangent nonlinear tracking differentiator (TANH-NTD) to estimate the interference of the system and enhance the robustness of the system. The stability of the system is proved by the Lyapunov principle. The numerical simulation results show that the method can shorten the system arrival time, improve the tracking accuracy, and suppress the chattering phenomenon.

## 1. Introduction

Sliding mode variable structure control is essentially a nonlinear control that the structure changes over time. Its significant advantage is its strong robustness to uncertain parameters and external disturbances. Therefore, it has been widely used in aerospace, robot control, and chemical control [1–8]. However, the traditional sliding mode control takes the linear sliding mode as the "sliding mode" of the system. The deviation between the system state and the given trajectory converges exponentially but cannot converge to zero in a finite time. Therefore, the nonlinear term is introduced in the design of terminal sliding mode (TSM) control, and the tracking error on the sliding mode surface can converge to zero in a limited time, which makes it widely used in various control systems [9–12]. Reference [13] proposed a terminal sliding mode control design scheme for uncertain dynamic systems with pure feedback form. In Reference [14], a new terminal sliding mode control design is proposed for the n-link rigid manipulator. Reference [15] proposed a new sliding mode control method for robot terminals. Reference [16] discussed the design of terminal sliding mode variable structure control for multi-input uncertain linear system. However, TSM has singularity [17–19]. Nonsingular terminal sliding mode (NTSM) control evolved on the basis of avoiding the TSM singularity problem. It avoids the control singular regions directly in the sliding mode design and preserves the finite time convergence characteristics of TSM [20–25]. In recent years, NTSM has developed rapidly. In [26], a continuous nonsingular terminal sliding mode control method was proposed for the suppression of mismatch interference. In [27], in order to realize the finite time tracking control of the axial position of the nonlinear thrust active magnetic bearing rotor, a robust nonsingular terminal sliding mode control system was proposed. In order to further improve the convergence speed of the sliding mode, a nonsingular fast terminal sliding mode (NFTSM) surface was designed. Reference [28] studied the fast finite time control of terminal sliding mode with nonlinear dynamics. In [29], a state-based nonsingular fast-terminal sliding mode controller was designed using direct instantaneous torque control. However, the system was often affected by the uncertainty of the model and the amount of interference, resulting in system chattering and even instability. In order to solve this problem, Reference [30] proposed a continuous nonsingular fast terminal sliding mode control scheme with extended state observer and tracking differentiator for second-order uncertain SISO nonlinear systems. In [31],

the stability and attitude control of a class of quadrotor systems with uncertainties and unknown disturbances were studied. A nonsingular fast terminal sliding mode attitude control scheme for tracking differentiators and extended state observers was proposed. However, the extended state observer has an initial differential peak problem. Document [32] proposes an NDO design method for underactuated robot arm control. In [33], the NDO is combined with the dynamic surface to design the moving wheel inverted pendulum controller. They have a good effect on the estimation of the disturbance, but both of them have the disadvantage of relying on the prior knowledge of the disturbance. However, it is difficult to obtain prior knowledge of disturbance in practice. Literature [34] proposed a nonlinear disturbance observer based on tracking differentiator, which overcomes the shortcomings of the literature [32, 33] need to know the prior knowledge of disturbance. At the same time, it has the advantages of simple structure, excellent estimation effect on disturbance, and suppression of measurement noise.

In this paper, to realize fast and stable tracking control for a class of second-order uncertain nonlinear systems, a nonsingular fast terminal sliding mode control strategy combining RBF network and disturbance observer is proposed. The contributions of this paper are as follows.

(1) The sliding mode controller is designed by using nonsingular fast terminal sliding mode and second power reaching law, so that the system can converge to zero smoothly in a short time.

(2) RBF neural networks have strong nonlinear fitting ability to map arbitrarily complex nonlinear relationships. At the same time, it has the advantages of simple learning rules and easy computer implementation. Using the universal approximation principle of RBF network, the unknown nonlinear function is approximated to solve the influence of unknown nonlinear function on the robustness of the system.

(3) The nonlinear disturbance observer based on tracking differentiator has the advantages of simple structure, good disturbance estimation effect, and suppressing measurement noise. A hyperbolic tangent nonlinear disturbance observer is designed to estimate the external disturbance and unknown part of the model and compensate the controller. At the same time, an augmented nonlinear tracking differentiator designed in Reference [35] is used to filter the given signal, eliminating the influence of the given noise on the system.

The numerical simulation results show that the designed control method can effectively shorten the convergence time, eliminate the noise of the given signal and the chattering phenomenon in the controller, and improve the control tracking accuracy.

## 2. Problem Description

Consider the following second-order uncertain nonlinear system:

$$\begin{aligned} \dot{x}_1 &= x_2 \\ \dot{x}_2 &= f(\boldsymbol{x}) + b(\boldsymbol{x})\, u + d(t) \\ y &= x_1 \end{aligned} \tag{1}$$

where $\boldsymbol{x} = [x_1, x_2]^T \in R^2$ is the state variable; $f(\boldsymbol{x})$ and $b(\boldsymbol{x})$ are the unknown nonlinear functions; $u \in R$ is the control input; $y \in R$ is the system output; $d(t)$ is the slow time-varying interference, and $|d(t)| \le D$, constant $D > 0$.

## 3. Main Results

The control objective of the system is to design a robust controller that enables accurate and fast tracking of the desired input signal even in the presence of model uncertainties and external disturbances. In order to reach the target, an NFTSM control scheme combining RBF network and disturbance observer is designed. The structure diagram of the system controller is shown in Figure 1.

*3.1. Nonsingular Fast Terminal Sliding Mode Control.* In order to solve the problem of singularity and slow convergence of traditional terminal sliding mode control, a novel nonsingular fast terminal sliding mode control method is proposed.

*3.1.1. Sliding Mode Design.* $x_d$ is set the given signal and is second derivable. The position and velocity tracking errors of the system are defined as $e_1 = x_1 - x_d$ and $e_2 = x_2 - \dot{x}_d$, respectively. The designed nonsingular fast terminal sliding mode is

$$s = e_1 + \alpha_1 |e_1|^{\gamma} \operatorname{sgn}(e_1) + \alpha_2 |e_2|^{q/p} \operatorname{sgn}(e_2) \tag{2}$$

where $\alpha_1$, $\alpha_2$ are positive real numbers; $q$, $p$ are odd integers, and $1 < q/p < 2$, $\gamma > q/p$. $e_1$ and $e_2$ do not have negative exponential terms, ensuring that the sliding mode $s$ based controller does not have singularity. When the system error state reaches the sliding mode ($s = 0$), the following equation can be obtained:

$$e_1 + \alpha_1 |e_1|^{\gamma} \operatorname{sgn}(e_1) + \alpha_2 |e_2|^{q/p} \operatorname{sgn}(e_2) = 0 \tag{3}$$

Substitute $\dot{e}_1 = e_2$ into (3), the following equation can be obtained:

$$\begin{aligned} \dot{e}_1 &= -\left(\frac{1}{\alpha_2}\right)^{p/q} \left(e_1 + \alpha_1 |e_1|^{\gamma} \operatorname{sgn}(e_1)\right)^{p/q} \\ &= -\left(\frac{1}{\alpha_2}\right)^{p/q} {e_1}^{p/q} \left(1 + \alpha_1 |e_1|^{\gamma-1}\right)^{p/q} \end{aligned} \tag{4}$$

Assume the time taken from $e_1(t_r) \neq 0$ to $e_1(t_r + t_s) = 0$ is $t_s$, and the following equation can be obtained through the time integrated on both sides of (4):

$$\begin{aligned} &\int_{e_1(t_r)}^{e_1(t_r+t_s)} \left(\frac{1}{e_1}\right)^{p/q} de_1 \\ &= -\int_{t_r}^{t_r+t_s} \left(\frac{1}{\alpha_2}\right)^{p/q} \left(1 + \alpha_1 |e_1|^{\gamma-1}\right)^{p/q} d\tau \\ &\le -\int_{t_r}^{t_r+t_s} \left(\frac{1}{\alpha_2}\right)^{p/q} d\tau \end{aligned} \tag{5}$$

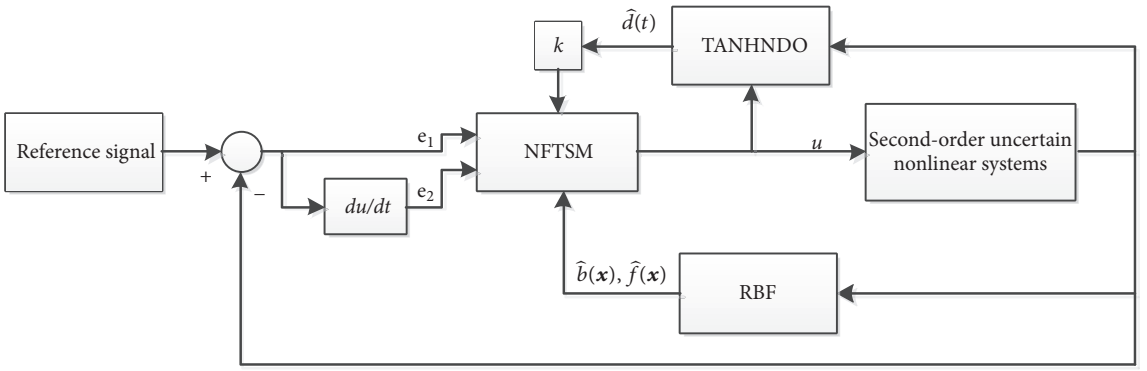


Figure 1: Structure diagram of the system controller.

*Simplification of Inequality (5)*

$$t_s \le \frac{\alpha_2^{p/q} q}{q-p} e_1 \left(t_r\right)^{1-p/q} \tag{6}$$

Therefore, the system error can converge to zero for a limited time.

*Remark 1.* When the system error state is far from the equilibrium point, the dominant role of $e_1$ in the sliding mode $s$ causes the system trajectory to converge quickly. When the system error state approaches the equilibrium point, the dominant role of $\alpha_1 |e_1|^{\gamma} \operatorname{sgn}(e_1)$ in the sliding mode $s$ causes the system trajectory to converge rapidly. Therefore, NFTSM can achieve fast convergence of the whole state trajectory.

*3.1.2. Reaching Law Design.* According to the sliding mode variable structure principle, the sliding mode reachability condition only ensures that the moving point at any position in the state space can reach the switching surface within a limited time, and there is no restriction on the specific trajectory of the reaching motion. The reaching law can improve the dynamic quality of reaching movement. The following second power reaching law is adopted in this paper.

$$\dot{s} = -k_3 |s|^{c_2} \operatorname{sgn}(s) - k_4 |s|^{c_3} \operatorname{sgn}(s) \tag{7}$$

where $k_3 > 0, k_4 > 0, 0 < c_2 < 1, c_3 > 1$. When the system state is far from the sliding mode ($|s| > 1$), $-k_4 |s|^{c_3} \operatorname{sgn}(s)$ plays a leading role; when the system approaches the sliding mode ($|s| < 1$), $-k_3 |s|^{c_2} \operatorname{sgn}(s)$ dominates. When $s = 0$, $\dot{s} = 0$, the speed of the state reaching the sliding mode is reduced to zero, and the smooth transition of the sliding mode is realized, which greatly weakens the system chattering phenomenon. Compared with the traditional power reaching law, exponential reaching law, and fast power reaching law, the reaching law (7) has faster convergence speed and better motion quality.

*3.1.3. Controller Design and Stability Analysis*

**Lemma 2** (see [36]). *Set $\boldsymbol{x} \in M \subset R^n$, $\dot{\boldsymbol{x}} = f(\boldsymbol{x})$, $f : R^n \longrightarrow R$ as the continuous functions defined in the equilibrium point region $M$. Assume that a continuous function $V : M \longrightarrow R$ satisfies the following conditions:*

*(1) $V$ is positive definite.*

*(2) $\dot{V}$ is negative definite except for the equilibrium point.*

*(3) Real number $k > 0$, $\alpha > 0$ and region $N \subset M$ make $\dot{V} + kV^{\alpha} \le 0$, and the function $\dot{\boldsymbol{x}} = f(\boldsymbol{x})$ converges at balanced zero point within finite time.*

**Theorem 3.** *For the system shown in (1), design the sliding mode according to (2), using the NFTSM controller shown in (9). The system state s converges to the following areas in a limited time:*

$$\begin{aligned} |s| &\le \min\left(\left(\frac{D}{k_3}\right)^{1/c_2}, \left(\frac{D}{k_4}\right)^{1/c_3}\right) \\ |\dot{s}| &\le \min\left(D, k_3\left(\frac{D}{k_4}\right)^{c_1/c_2}\right) \\ &\quad + \min\left(k_4\left(\frac{D}{k_3}\right)^{c_2/c_1}, D\right) \end{aligned} \tag{8}$$

*Sliding mode controller is designed as*

$$\begin{aligned} u = -b(\boldsymbol{x})^{-1} \Bigg[ & f(\boldsymbol{x}) \\ & + \frac{1}{\alpha_2} \frac{p}{q} |e_2|^{2-q/p} \operatorname{sgn}(e_2) \left(1 + \alpha_1 \gamma |e_1|^{\gamma-1}\right) \\ & + k_3 |s|^{c_2} \operatorname{sgn}(s) + k_4 |s|^{c_3} \operatorname{sgn}(s) - \ddot{x}_d \Bigg] \end{aligned} \tag{9}$$

*where $\alpha_1, \alpha_2, k_3, k_4$ are normal numbers, $0 < c_2 < 1, c_3 > 1$; $q$, $p$ are odd integers, and $1 < q/p < 2$, $\gamma > q/p$.*

*Proof.* Define the following Lyapunov function:

$$V = \frac{1}{2} s^2 \tag{10}$$

Find the time derivative for (10):

$$\begin{aligned}\dot{V} &= s\left(\dot{e}_1 + \alpha_1\gamma\left|e_1\right|^{\gamma-1}\operatorname{sgn}\left(e_1\right)\dot{e}_1\right.\\ &\quad\left.+\alpha_2\frac{q}{p}\left|e_2\right|^{q/p-1}\operatorname{sgn}\left(e_2\right)\dot{e}_2\right) = s\left(e_2\right.\\ &\quad\left.+\alpha_1\gamma\left|e_1\right|^{\gamma-1}\operatorname{sgn}\left(e_1\right)e_2+\alpha_2\frac{q}{p}\left|e_2\right|^{q/p-1}\operatorname{sgn}\left(e_2\right)\right.\\ &\quad\left.\cdot\left(f\left(\boldsymbol{x}\right)+b\left(\boldsymbol{x}\right)u+d\left(t\right)-\ddot{x}_d\right)\right)\end{aligned} \tag{11}$$

Substitute (9) into the above equation:

$$\begin{aligned}\dot{V} &= s\left(\dot{e}_1+\alpha_1\gamma\left|e_1\right|^{\gamma-1}\dot{e}_1+\alpha_2\frac{q}{p}\left|e_2\right|^{q/p-1}\dot{e}_2\right)\\ &= s\left(e_2+\alpha_1\gamma\left|e_1\right|^{\gamma-1}e_2+\alpha_2\frac{q}{p}\left|e_2\right|^{q/p-1}\left(f\left(\boldsymbol{x}\right)+b\left(\boldsymbol{x}\right)\left(-b\left(\boldsymbol{x}\right)^{-1}\right.\right.\right.\\ &\quad\cdot\left[f\left(\boldsymbol{x}\right)+\frac{1}{\alpha_2}\frac{p}{q}\left|e_2\right|^{2-q/p}\operatorname{sgn}\left(e_2\right)\left(1+\alpha_1\gamma\left|e_1\right|^{\gamma-1}\right)\right.\\ &\quad\left.+k_3\left|s\right|^{c_2}\operatorname{sgn}\left(s\right)+k_4\left|s\right|^{c_3}\operatorname{sgn}\left(s\right)-\ddot{x}_d\right]\Big)+d\left(t\right)\\ &\quad\left.\left.-\ddot{x}_d\right)\right)\end{aligned} \tag{12}$$

$$\begin{aligned}&= s\left(\alpha_2\frac{q}{p}\left|e_2\right|^{q/p-1}\left(-k_3\left|s\right|^{c_2}\operatorname{sgn}\left(s\right)-k_4\left|s\right|^{c_3}\operatorname{sgn}\left(s\right)+d\left(t\right)\right)\right)\\ &= -\alpha_2\frac{q}{p}\left|e_2\right|^{q/p-1}\left(k_3\left|s\right|^{c_2+1}+k_4\left|s\right|^{c_3+1}-sd\left(t\right)\right)\\ &\le -\alpha_2\frac{q}{p}\left|e_2\right|^{q/p-1}\left(k_3\left|s\right|^{c_2+1}+k_4\left|s\right|^{c_3+1}-D\left|s\right|\right)\end{aligned}$$

Deform (12):

$$\begin{aligned}\dot{V} &\le -\alpha_2\frac{q}{p}\left|e_2\right|^{q/p-1}k_3\left|s\right|^{c_2+1}-\alpha_2\frac{q}{p}\left|e_2\right|^{q/p-1}k_4\left|s\right|^{c_3+1}\\ &\quad+\alpha_2\frac{q}{p}\left|e_2\right|^{q/p-1}D\left|s\right|\\ &= -\alpha_2\frac{q}{p}\left|e_2\right|^{q/p-1}k_3\left|s\right|^{c_2+1}\\ &\quad-\left|s\right|\alpha_2\frac{q}{p}\left|e_2\right|^{q/p-1}\left(k_4\left|s\right|^{c_3}-D\right)\end{aligned} \tag{13}$$

Because $\alpha_2$ is a normal number, $c_3 > 1$; $q$, $p$ are odd integers, and $1 < q/p < 2$, so $\alpha_2(q/p)|e_2|^{q/p-1} \ge 0$. If $k_4|s|^{c_3} - D \ge 0$, then (13) can be further changed to

$$\begin{aligned}\dot{V} &\le -\alpha_2\frac{q}{p}\left|e_2\right|^{q/p-1}k_3\left|s\right|^{c_2+1}\\ &= -\alpha_2\frac{q}{p}\left|e_2\right|^{q/p-1}k_3V^{(c_2+1)/2}\end{aligned} \tag{14}$$

Also, because $k_3 > 0$, $0 < c_2 < 1$, that is, $\alpha_2(q/p)|e_2|^{q/p-1}k_3 > 0$, $(c_2+1)/2 > 0$, (14) satisfies Lemma 2, and the system converges on the finite time of the equilibrium zero and can ensure the convergence of the following regions in a finite time.

$$\left|s\right| \le \left(\frac{D}{k_4}\right)^{1/c_3} \tag{15}$$

Similarly, equation (12) can be transformed into

$$\begin{aligned}\dot{V} &\le -\alpha_2\frac{q}{p}\left|e_2\right|^{q/p-1}k_4\left|s\right|^{c_3+1}\\ &\quad-\left|s\right|\alpha_2\frac{q}{p}\left|e_2\right|^{q/p-1}\left(k_3\left|s\right|^{c_2}-D\right)\end{aligned} \tag{16}$$

Because $\alpha_2(q/p)|e_2|^{q/p-1} \ge 0$, if $k_3|s|^{c_2} - D \ge 0$, then (16) can be further changed to

$$\begin{aligned}\dot{V} &\le -\alpha_2\frac{q}{p}\left|e_2\right|^{q/p-1}k_4\left|s\right|^{c_3+1}\\ &= -\alpha_2\frac{q}{p}\left|e_2\right|^{q/p-1}k_4V^{(c_3+1)/2}\end{aligned} \tag{17}$$

Also, because $\alpha_2(q/p)|e_2|^{q/p-1}k_3 > 0$, $c_3 > 1$, $(c_3+1)/2 > 0$, (17) satisfies Lemma 2, and the system converges on the finite time to the equilibrium zero and can guarantee the convergence of the following regions in a finite time.

$$\left|s\right| \le \left(\frac{D}{k_3}\right)^{1/c_2} \tag{18}$$

Combining equations (15) and (18), the system state $s$ converges to the following areas within a limited time:

$$\left|s\right| \le \min\left(\left(\frac{D}{k_3}\right)^{1/c_2},\left(\frac{D}{k_4}\right)^{1/c_3}\right) \tag{19}$$

Substituting the previous equation into (7), we can get

$$\begin{aligned}\left|\dot{s}\right| &\le k_3\left|s\right|^{c_2}\operatorname{sgn}\left(s\right)+k_4\left|s\right|^{c_3}\operatorname{sgn}\left(s\right)\\ &\le k_3\left|s\right|^{c_2}+k_4\left|s\right|^{c_3}\\ &\le k_3\cdot\min\left(\left(\frac{D}{k_3}\right)^{1/c_2},\left(\frac{D}{k_4}\right)^{1/c_3}\right)^{c_2}+k_4\\ &\quad\cdot\min\left(\left(\frac{D}{k_3}\right)^{1/c_2},\left(\frac{D}{k_4}\right)^{1/c_3}\right)^{c_3}\\ &= \min\left(D,k_3\left(\frac{D}{k_4}\right)^{c_1/c_2}\right)\\ &\quad+\min\left(k_4\left(\frac{D}{k_3}\right)^{c_2/c_1},D\right)\end{aligned} \tag{20}$$

Theorem 3 is proved. □

*3.2. RBF Network Approximation $f(\boldsymbol{x})$ and $b(\boldsymbol{x})$.* The nonlinear functions $f(\boldsymbol{x})$ and $b(\boldsymbol{x})$ are required according to the control law (9), but the actual control needs to be obtained based on empirical knowledge, and sometimes it is not available. Therefore, it is approximated by the approximation principle. Because the RBF neural network has strong nonlinear fitting ability, it can map arbitrarily complex nonlinear relationships. At the same time, it has the advantages of simple learning rules and easy computer implementation. Therefore, using the universal approximation principle of RBF network, the unknown nonlinear function is approximated to solve the problem of the acquisition of unknown nonlinear function in the control law and the influence of unknown nonlinear function on the robustness of the system.

*3.2.1. RBF Neural Network Structure.* The RBF network is a 3-layer forward network with a simple structure and is suitable for real-time control. The structure of the RBF network with multiple inputs and single output is shown in Figure 2.

In the RBF network, $\boldsymbol{x} = [x_1 \ \ x_2 \ \ \cdots \ \ x_n]^T$ is the network input, and $h_j$ is the Gaussian function, which represents the output of the $j$th neuron in the hidden layer; namely,

$$h_j = \exp\left(-\frac{\left\|\boldsymbol{x} - \boldsymbol{c}_j\right\|^2}{2g_j^2}\right), \quad j = 1, 2, \cdots, m \tag{21}$$

where $\boldsymbol{c}_j = [c_{j1}, c_{j2}, \cdots, c_{jm}]$ is the center of the Gaussian function of the node $j$; $g_j$ is the width of the Gaussian function of the node $j$. The weight of the network is taken as $\boldsymbol{\theta} = [\theta_1, \theta_2, \cdots, \theta_m]^T$.

Output of RBF network is

$$y_m(t) = \theta_1 h_1 + \theta_2 h_2 + \cdots + \theta_m h_m \tag{22}$$

*3.2.2. Adaptive Approximation of RBF Network.* For the unknown nonlinear functions $f(\boldsymbol{x})$ and $b(\boldsymbol{x})$ in (9), the RBF network adaptive approximation is adopted. The RBF network input and output algorithm is

$$\begin{aligned} h_j &= \exp\left(-\frac{\left\|\boldsymbol{x} - \boldsymbol{c}_j\right\|^2}{2g_j^2}\right), \quad j = 1, 2, \cdots, m \\ f(\boldsymbol{x}) &= \boldsymbol{W}^{*T}\boldsymbol{h}_f(\boldsymbol{x}) + \varepsilon_f, \\ b(\boldsymbol{x}) &= \boldsymbol{V}^{*T}\boldsymbol{h}_b(\boldsymbol{x}) + \varepsilon_b \end{aligned} \tag{23}$$

where $\boldsymbol{x}$ is the network input; $h_j$ is the Gaussian function; $\boldsymbol{W}^*$ and $\boldsymbol{V}^*$ are the ideal network weight vectors of $f(\boldsymbol{x})$ and $b(\boldsymbol{x})$, respectively; $\varepsilon_f$ and $\varepsilon_b$ are the network approximation errors, $|\varepsilon_f| \le \varepsilon_{Mf}$, $|\varepsilon_b| \le \varepsilon_{Mb}$. $\boldsymbol{h}_f(\boldsymbol{x})$, $\boldsymbol{h}_b(\boldsymbol{x})$ are vector functions, and the elements of them are all Gaussian function. We can set $\boldsymbol{x} = [x_1 \ \ x_2]^T$, and then the output of the RBF network is

$$\begin{aligned} \widehat{f}(\boldsymbol{x}) &= \widehat{\boldsymbol{W}}^T\boldsymbol{h}_f(\boldsymbol{x}), \\ \widehat{b}(\boldsymbol{x}) &= \widehat{\boldsymbol{V}}^T\boldsymbol{h}_b(\boldsymbol{x}) \end{aligned} \tag{24}$$

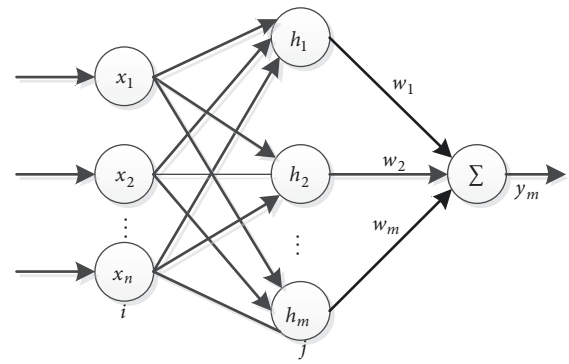


Figure 2: The RBF network with multiple inputs and single output.

Design control law is

$$\begin{aligned} u = -\widehat{b}(\boldsymbol{x})^{-1}\Bigg[&\widehat{f}(\boldsymbol{x}) \\ &+ \frac{1}{\alpha_2}\frac{p}{q}|e_2|^{2-q/p}\operatorname{sgn}(e_2)\left(1 + \alpha_1\gamma|e_1|^{\gamma-1}\right) \\ &+ k_3|s|^{c_2}\operatorname{sgn}(s) + k_4|s|^{c_3}\operatorname{sgn}(s) - \ddot{x}_d\Bigg] \end{aligned} \tag{25}$$

where $\alpha_1, \alpha_2, k_3, k_4$ are normal numbers, and $0 < c_2 < 1$, $c_3 > 1$. $q$, $p$ are odd integers, and $1 < q/p < 2$, $\gamma > q/p$. $\widehat{f}(\boldsymbol{x})$ and $\widehat{b}(\boldsymbol{x})$ are the RBF network output values.

Find the time derivative for (2):

$$\begin{aligned} \dot{s} = \dot{e}_1 + \alpha_1\gamma|e_1|^{\gamma-1}e_2 + \alpha_2\frac{q}{p}|e_2|^{q/p-1}\dot{e}_2 = \Bigg(&e_2 \\ &+ \alpha_1\gamma|e_1|^{\gamma-1}e_2 + \alpha_2\frac{q}{p}|e_2|^{q/p-1}\left(f(\boldsymbol{x}) + b(\boldsymbol{x})u\right. \\ &\left.+ d(t) - \ddot{x}_d\right)\Bigg) = \Bigg(e_2 + \alpha_1\gamma|e_1|^{\gamma-1}e_2 + \alpha_2 \\ &\cdot\frac{q}{p}|e_2|^{q/p-1}\left(f(\boldsymbol{x}) + \widehat{b}(\boldsymbol{x})u + \left(b(\boldsymbol{x}) - \widehat{b}(\boldsymbol{x})\right)u\right. \\ &\left.+ d(t) - \ddot{x}_d\right)\Bigg) \end{aligned} \tag{26}$$

Substitute (25) into (26):

$$\begin{aligned} \dot{s} = e_2 + \alpha_1\gamma|e_1|^{\gamma-1}e_2 + \alpha_2\frac{q}{p}|e_2|^{q/p-1}\Bigg(&f(\boldsymbol{x}) + \widehat{b}(\boldsymbol{x}) \\ &\cdot\Bigg(-\widehat{b}(\boldsymbol{x})^{-1}\Bigg[\widehat{f}(\boldsymbol{x}) \\ &+ \frac{1}{\alpha_2}\frac{p}{q}|e_2|^{2-q/p}\operatorname{sgn}(e_2)\left(1 + \alpha_1\gamma|e_1|^{\gamma-1}\right) \\ &+ k_3|s|^{c_2}\operatorname{sgn}(s) + k_4|s|^{c_3}\operatorname{sgn}(s) - \ddot{x}_d\Bigg]\Bigg) + \left(b(\boldsymbol{x})\right. \\ &\left.- \widehat{b}(\boldsymbol{x})\right)u + d(t) - \ddot{x}_d\Bigg) = \alpha_2\frac{q}{p}|e_2|^{q/p-1}\left(f(\boldsymbol{x})\right. \\ &\left.- \widehat{f}(\boldsymbol{x}) - k_3|s|^{c_2}\operatorname{sgn}(s) - k_4|s|^{c_3}\operatorname{sgn}(s) + \left(b(\boldsymbol{x})\right.\right. \end{aligned}$$

$$
\begin{aligned}
&- \widehat{b}(\boldsymbol{x})\big)u + d(t)\big) = \alpha_2 \frac{q}{p} |e_2|^{q/p-1} \left(\widetilde{f}(\boldsymbol{x}) - k_3 |s|^{c_2}\right. \\
&\cdot \operatorname{sgn}(s) - k_4 |s|^{c_3} \operatorname{sgn}(s) + \widetilde{b}(\boldsymbol{x})u + d(t)\big) = \alpha_2 \\
&\cdot \frac{q}{p} |e_2|^{q/p-1} \left(\widetilde{\boldsymbol{W}}^T \boldsymbol{h}_f(\boldsymbol{x}) - \varepsilon_f - k_3 |s|^{c_2} \operatorname{sgn}(s)\right. \\
&- k_4 |s|^{c_3} \operatorname{sgn}(s) + \left(\widetilde{\boldsymbol{V}}^T \boldsymbol{h}_b(\boldsymbol{x}) - \varepsilon_b\right)u + d(t)\Big)
\end{aligned} \tag{27}
$$

where $\widetilde{\boldsymbol{W}} = \widehat{\boldsymbol{W}} - \boldsymbol{W}^*$, $\widetilde{\boldsymbol{V}} = \widehat{\boldsymbol{V}} - \boldsymbol{V}^*$, and

$$
\begin{aligned}
\widetilde{f} &= f - \widehat{f} = \boldsymbol{W}^{*T} \boldsymbol{h}_f(\boldsymbol{h}) - \widehat{\boldsymbol{W}}^T \boldsymbol{h}_f(\boldsymbol{x}) - \varepsilon_f \\
&= \widetilde{\boldsymbol{W}}^T \boldsymbol{h}_f(\boldsymbol{x}) - \varepsilon_f \\
\widetilde{b} &= b - \widehat{b} = \boldsymbol{V}^{*T} \boldsymbol{h}_b(\boldsymbol{x}) - \widehat{\boldsymbol{V}}^T \boldsymbol{h}_b(\boldsymbol{x}) - \varepsilon_b \\
&= \widetilde{\boldsymbol{V}}^T \boldsymbol{h}_b(\boldsymbol{x}) - \varepsilon_b
\end{aligned} \tag{28}
$$

Design the Lyapunov function as

$$
L = \frac{1}{2}s^2 + \frac{1}{2r_1}\widetilde{\boldsymbol{W}}^T\widetilde{\boldsymbol{W}} + \frac{1}{2r_2}\widetilde{\boldsymbol{V}}^T\widetilde{\boldsymbol{V}} \tag{29}
$$

where $r_1 > 0$, $r_2 > 0$.
Find the time derivative for (29) and substitute it into (27):

$$
\begin{aligned}
\dot{L} &= s\alpha_2 \frac{q}{p} |e_2|^{q/p-1} \left(\widetilde{\boldsymbol{W}}^T \boldsymbol{h}_f(\boldsymbol{x}) - \varepsilon_f - k_3 |s|^{c_2} \operatorname{sgn}(s)\right. \\
&- k_4 |s|^{c_3} \operatorname{sgn}(s) + \left(\widetilde{\boldsymbol{V}}^T \boldsymbol{h}_b(\boldsymbol{x}) - \varepsilon_b\right)u + d(t)\Big) + \frac{1}{r_1} \\
&\cdot \widetilde{\boldsymbol{W}}^T \dot{\widehat{\boldsymbol{W}}} + \frac{1}{r_2}\widetilde{\boldsymbol{V}}^T \dot{\widehat{\boldsymbol{V}}} = \widetilde{\boldsymbol{W}}^T \left(\alpha_2 \frac{q}{p} |e_2|^{q/p-1} s\boldsymbol{h}_f(\boldsymbol{x})\right. \\
&+ \frac{1}{r_1}\dot{\widehat{\boldsymbol{W}}}\Big) + \widetilde{\boldsymbol{V}}^T \left(\alpha_2 \frac{q}{p} |e_2|^{q/p-1} s\boldsymbol{h}_b(\boldsymbol{x})u + \frac{1}{r_2}\dot{\widehat{\boldsymbol{V}}}\right) \\
&+ \alpha_2 \frac{q}{p} |e_2|^{q/p-1} s\left(-\varepsilon_f - k_3 |s|^{c_2} \operatorname{sgn}(s)\right. \\
&- k_4 |s|^{c_3} \operatorname{sgn}(s) - \varepsilon_b u + d(t)\Big)
\end{aligned} \tag{30}
$$

Take the adaptive law as

$$
\begin{aligned}
\dot{\widehat{\boldsymbol{W}}} &= -r_1\alpha_2 \frac{q}{p} |e_2|^{q/p-1} s\boldsymbol{h}_f(\boldsymbol{x}) \\
\dot{\widehat{\boldsymbol{V}}} &= -r_2\alpha_2 \frac{q}{p} |e_2|^{q/p-1} s\boldsymbol{h}_b(\boldsymbol{x})u
\end{aligned} \tag{31}
$$

Substitute (31) into (30):

$$
\begin{aligned}
\dot{L} &= \alpha_2 \frac{q}{p} |e_2|^{q/p-1} s\left(-\varepsilon_f - k_3 |s|^{c_2} \operatorname{sgn}(s)\right. \\
&- k_4 |s|^{c_3} \operatorname{sgn}(s) - \varepsilon_b u + d(t)\Big) = -\alpha_2 \frac{q}{p} |e_2|^{q/p-1} \\
&\cdot \left(k_3 |s|^{c_2+1} + k_4 |s|^{c_3+1} + s\left(\varepsilon_f + \varepsilon_b u - d(t)\right)\right) \\
&\le -\alpha_2 \frac{q}{p} |e_2|^{q/p-1} \left(k_3 |s|^{c_2+1} + k_4 |s|^{c_3+1}\right. \\
&+ |s|\left(\varepsilon_f + \varepsilon_b u - D\right)\Big)
\end{aligned} \tag{32}
$$

Since $\varepsilon_f$ and $\varepsilon_b$, the RBF network approximation errors, are very small real numbers, $\delta$ is selected as $\delta \ge |\varepsilon_f + \varepsilon_b u - D|$. According to Theorem 3, the system state $s$ converges to the following region within a finite time:

$$
\begin{aligned}
|s| &\le \min\left(\left(\frac{\delta}{k_3}\right)^{1/c_2}, \left(\frac{\delta}{k_4}\right)^{1/c_3}\right) \\
|\dot{s}| &\le \min\left(\delta, k_3\left(\frac{\delta}{k_4}\right)^{c_1/c_2}\right) \\
&\quad + \min\left(k_4\left(\frac{\delta}{k_3}\right)^{c_2/c_1}, \delta\right)
\end{aligned} \tag{33}
$$

*3.3. Hyperbolic Tangent Nonlinear Disturbance Observer.* For system (1), the interference of the system is not only the model unknown interference generated by the unknown nonlinear function, but also the external disturbance. However, from (33), an important condition for the system state $s$ to reach the convergence region in a finite time is that the disturbance amount $d(t)$ in (1) is $|d(t)| \le D$ and $D$ is affected by the disturbance amount $d(t)$. When $d(t)$ is larger, $D$ becomes larger, which affects the stability of the system. In order to further eliminate the influence of the interference amount on the control system, the nonlinear disturbance observer using the tracking-differentiator has the advantages of simple structure, good interference estimation effect, suppression of measurement noise, etc., and a hyperbolic tangent nonlinear disturbance observer is designed. The interference in (1) is estimated and feedforward compensation is performed to improve the anti-interference ability of the system.

**Lemma 4** (see [37]). *Consider the following system* $\Sigma_1$*:*

$$
\begin{aligned}
\dot{z}_1 &= z_2(t) \\
\dot{z}_2 &= -a_1 \tanh\left(b_1 z_1(t)\right) - a_2 \tanh\left(b_2 z_2(t)\right)
\end{aligned} \tag{34}
$$

*If* $a_1$, $a_2$, $b_1$, $b_2$ *are all positive real numbers, the system* $\Sigma_1$ *is progressively stable at the origin* $(0, 0)$*. It satisfies*

$$
\begin{aligned}
\lim_{t\to\infty} z_1(t) &= 0 \\
\lim_{t\to\infty} z_2(t) &= 0
\end{aligned} \tag{35}
$$

*An improved disturbance observer is designed by using the hyperbolic tangent tracking differentiator proposed in [37].*

$$\begin{aligned}\dot{\hat{x}}_2 &= f(\boldsymbol{x}) + b(\boldsymbol{x})u + \hat{d}\\ \dot{\hat{d}} &= -R^2\left[a_1\tanh\left(b_1\left(\hat{x}_2 - x_2\right)\right) + a_2\tanh\left(\frac{b_2\hat{d}}{R}\right)\right]\end{aligned} \tag{36}$$

*In the formula, $R$, $a_1$, $a_2$, $b_1$, $b_2$ are all positive real numbers; $\hat{\boldsymbol{x}}$ and $\hat{d}$ are, respectively, estimates of $\boldsymbol{x}$ and $d$. If $T > 0$, $R > 0$, there are*

$$\lim_{R\longrightarrow\infty}\int_0^T \left|\hat{x}_2 - x_2\right| dt = 0 \tag{37}$$

*When $R \longrightarrow \infty$, it can be obtained that $|\dot{\hat{d}}| = |-R^2[a_1\tanh(b_1(\hat{x}_2 - x_2)) + a_2\tanh(b_2\hat{d}/R)]|$ gets closer to infinity, so $\hat{d}$ changes faster than $f(\boldsymbol{x}) + b(\boldsymbol{x})u$; that is, $\lim_{R\longrightarrow\infty} d(f(\boldsymbol{x}) + b(\boldsymbol{x})u + \hat{d})/dt = \dot{\hat{d}}$. Therefore, (36) satisfy Lemma 4, and the designed disturbance observer is progressively stable.*

*For (1), the following control laws are used:*

$$\begin{aligned}u = -\hat{b}(\boldsymbol{x})^{-1}\Bigg[&\hat{f}(\boldsymbol{x}) + k\hat{d}(t)\\ &+ \frac{1}{\alpha_2}\frac{p}{q}\left|e_2\right|^{2-q/p}\operatorname{sgn}(e_2)\left(1 + \alpha_1\gamma\left|e_1\right|^{\gamma-1}\right)\\ &+ k_3\left|s\right|^{c_2}\operatorname{sgn}(s) + k_4\left|s\right|^{c_3}\operatorname{sgn}(s) - \ddot{x}_d\Bigg]\end{aligned} \tag{38}$$

*where $\alpha_1$, $\alpha_2$, $k_3$, $k_4$, $k$ are normal numbers, $0 < c_2 < 1$, $c_3 > 1$. $q$ and $p$ are odd integers, and $1 < q/p < 2$, $\gamma > q/p$. $\hat{f}(\boldsymbol{x})$ and $\hat{b}(\boldsymbol{x})$ are the output values of the RBF network. $\hat{d}(t)$ is the output value of the hyperbolic tangent nonlinear disturbance observer. The system state $s$ will converge to a smaller region for a limited time.*

*Take a derivative of function (29) according to the Lyapunov, combining with (26), (31), and (38):*

$$\begin{aligned}\dot{L}&\\ &= s\Bigg(e_2 + \alpha_1\gamma\left|e_1\right|^{\gamma-1}e_2 + \alpha_2\frac{q}{p}\left|e_2\right|^{q/p-1}\Bigg(f(\boldsymbol{x}) + \hat{b}(\boldsymbol{x})\Bigg(-\hat{b}(\boldsymbol{x})^{-1}\\ &\cdot\Bigg[\hat{f}(\boldsymbol{x}) + k\hat{d}(t) + \frac{1}{\alpha_2}\frac{p}{q}\left|e_2\right|^{2-q/p}\operatorname{sgn}(e_2)\\ &\cdot\left(1 + \alpha_1\gamma\left|e_1\right|^{\gamma-1}\right) + k_3\left|s\right|^{c_2}\operatorname{sgn}(s) + k_4\left|s\right|^{c_3}\operatorname{sgn}(s)\\ &- \ddot{x}_d\Bigg]\Bigg) + \left(b(\boldsymbol{x}) - \hat{b}(\boldsymbol{x})\right)u + d(t) - \ddot{x}_d\Bigg)\Bigg) + \frac{1}{r_1}\\ &\cdot\widetilde{\boldsymbol{W}}^T\dot{\hat{\boldsymbol{W}}} + \frac{1}{r_2}\widetilde{\boldsymbol{V}}^T\dot{\hat{\boldsymbol{V}}}\\ &= s\alpha_2\frac{q}{p}\left|e_2\right|^{q/p-1}\left(\widetilde{\boldsymbol{W}}^T\boldsymbol{h}_f(\boldsymbol{x})\right.\\ &- \varepsilon_f - k\hat{d}(t) - k_3\left|s\right|^{c_2}\operatorname{sgn}(s) - k_4\left|s\right|^{c_3}\operatorname{sgn}(s) + \left(\widetilde{\boldsymbol{V}}^T\boldsymbol{h}_b(\boldsymbol{x})\right.\\ &\left.\left.- \varepsilon_b\right)u + d(t)\right) + \frac{1}{r_1}\widetilde{\boldsymbol{W}}^T\dot{\hat{\boldsymbol{W}}} + \frac{1}{r_2}\widetilde{\boldsymbol{V}}^T\dot{\hat{\boldsymbol{V}}}\\ &= \widetilde{\boldsymbol{W}}^T\Bigg(\alpha_2\\ &\cdot\frac{q}{p}\left|e_2\right|^{q/p-1}s\boldsymbol{h}_f(\boldsymbol{x}) + \frac{1}{r_1}\dot{\hat{\boldsymbol{W}}}\Bigg)\\ &+ \widetilde{\boldsymbol{V}}^T\Bigg(\alpha_2\\ &\cdot\frac{q}{p}\left|e_2\right|^{q/p-1}s\boldsymbol{h}_b(\boldsymbol{x})u + \frac{1}{r_2}\dot{\hat{\boldsymbol{V}}}\Bigg)\\ &+ \alpha_2\frac{q}{p}\left|e_2\right|^{q/p-1}\\ &\cdot s\left(-\varepsilon_f - k_3\left|s\right|^{c_2}\operatorname{sgn}(s) - k_4\left|s\right|^{c_3}\operatorname{sgn}(s) - \varepsilon_b u - k\hat{d}(t) + d(t)\right)\\ &= \alpha_2\frac{q}{p}\left|e_2\right|^{q/p-1}\\ &\cdot s\left(-\varepsilon_f - k_3\left|s\right|^{c_2}\operatorname{sgn}(s) - k_4\left|s\right|^{c_3}\operatorname{sgn}(s) - \varepsilon_b u - k\hat{d}(t) + d(t)\right)\\ &= -\alpha_2\frac{q}{p}\left|e_2\right|^{q/p-1}\left(k_3\left|s\right|^{c_2+1} + k_4\left|s\right|^{c_3+1}\right)\\ &+ s\left(\varepsilon_f + \varepsilon_b u + k\hat{d}(t) - d(t)\right)\\ &\le -\alpha_2\frac{q}{p}\left|e_2\right|^{q/p-1}\left(k_3\left|s\right|^{c_2+1} + k_4\left|s\right|^{c_3+1}\right)\\ &+ \left|s\right|\left(\varepsilon_f + \varepsilon_b u + k\hat{d}(t) - D\right)\end{aligned} \tag{39}$$

*Setting $\delta' \ge |\varepsilon_f + \varepsilon_b u + k\hat{d}(t) - D|$, according to Theorem 3, the system state $s$ converges to the following region within a finite time:*

$$\begin{aligned}\left|s\right| &\le \min\left(\left(\frac{\delta'}{k_3}\right)^{1/c_2}, \left(\frac{\delta'}{k_4}\right)^{1/c_3}\right)\\ \left|\dot{s}\right| &\le \min\left(\delta', k_3\left(\frac{\delta'}{k_4}\right)^{c_1/c_2}\right)\\ &+ \min\left(k_4\left(\frac{\delta'}{k_3}\right)^{c_2/c_1}, \delta'\right)\end{aligned} \tag{40}$$

**Theorem 5.** *For the system shown in (1), design the sliding mode according to (2), using the NFTSM controller shown in (38). The system state converges to the following areas in a limited time:*

$$\begin{aligned}\left|e_1\right| &\le \min\left(\left(\frac{\delta'}{k_3{\alpha_1}^{c_2}}\right)^{1/\gamma c_2}, \left(\frac{\delta'}{k_4{\alpha_1}^{c_3}}\right)^{1/\gamma c_3}\right)\\ \left|e_2\right| &\le \min\left(\left(\frac{\delta'}{k_3{\alpha_2}^{c_2}}\right)^{p/(qc_2)}, \left(\frac{\delta'}{k_4{\alpha_2}^{c_3}}\right)^{p/(qc_3)}\right)\end{aligned} \tag{41}$$

*Proof.* According to Theorem 3 and (40), system state enters $|s| \le \min((\delta'/k_3)^{1/c_2}, (\delta'/k_4)^{1/c_3})$ region, and we can get

$$e_1 + \alpha_1\left|e_1\right|^{\gamma}\operatorname{sgn}(e_1) + \alpha_2\left|e_2\right|^{q/p}\operatorname{sgn}(e_2) = \sigma \tag{42}$$

where $|\sigma| \in \Omega_s = \{s \mid |s| \le \min((\delta'/k_3)^{1/c_2}, (\delta'/k_4)^{1/c_3})\}$.

Equation (42) can be changed to

$$e_1 + \alpha_1 |e_1|^{\gamma} \operatorname{sgn}(e_1) + \left(\alpha_2 - \frac{\sigma}{|e_2|^{q/p} \operatorname{sgn}(e_2)}\right) |e_2|^{q/p} \operatorname{sgn}(e_2) = 0 \tag{43}$$

When $\alpha_2 - \sigma/|e_2|^{q/p} \operatorname{sgn}(e_2) > 0$, (43) satisfies the NFTSM form described in (2), and the system trajectory will converge to

$$\alpha_2 \le \frac{\sigma}{|e_2|^{q/p} \operatorname{sgn}(e_2)} \tag{44}$$

Therefore, state $e_2$ can converge rapidly to the region within a finite time $t_s$:

$$\begin{aligned} |e_2| &\le \left(\frac{\sigma}{\alpha_2}\right)^{p/q} \\ &\le \left(\frac{\min\left(\left(\delta'/k_3\right)^{1/c_2}, \left(\delta'/k_4\right)^{1/c_3}\right)}{\alpha_2}\right)^{p/q} \\ &\le \min\left(\left(\frac{\delta'}{k_3\alpha_2^{c_2}}\right)^{p/(qc_2)}, \left(\frac{\delta'}{k_4\alpha_2^{c_3}}\right)^{p/(qc_3)}\right) \end{aligned} \tag{45}$$

$$t_s \le \frac{\left(\alpha_2 - \sigma/|e_2|^{q/p} \operatorname{sgn}(e_2)\right)^{p/q} q}{q-p} e_1(t_r)^{1-p/q} \tag{46}$$

Using the same approach, (42) can be changed to

$$e_1 + \left(\alpha_1 - \frac{\sigma}{|e_1|^{\gamma} \operatorname{sgn}(e_1)}\right) |e_1|^{\gamma} \operatorname{sgn}(e_1) + \alpha_2 |e_2|^{q/p} \operatorname{sgn}(e_2) = 0 \tag{47}$$

When $\alpha_1 - \sigma/|e_1|^{\gamma} \operatorname{sgn}(e_1) > 0$, (47) satisfies the NFTSM form described in (2), and the system trajectory will converge to

$$\alpha_1 \le \frac{\sigma}{|e_1|^{\gamma} \operatorname{sgn}(e_1)} \tag{48}$$

Therefore, state $e_1$ can converge rapidly to the region within a finite time $t_s$:

$$\begin{aligned} |e_1| &\le \left(\frac{\sigma}{\alpha_1}\right)^{\gamma} \\ &\le \left(\frac{\min\left(\left(\delta'/k_3\right)^{1/c_2}, \left(\delta'/k_4\right)^{1/c_3}\right)}{\alpha_1}\right)^{\gamma} \\ &\le \min\left(\left(\frac{\delta'}{k_3\alpha_1^{c_2}}\right)^{1/\gamma c_2}, \left(\frac{\delta'}{k_4\alpha_1^{c_3}}\right)^{1/\gamma c_3}\right) \end{aligned} \tag{49}$$

Theorem 5 is proved. □

*Remark 6.* As the amount of disturbance $d(t)$ in (1) becomes larger, $D$ and $\widehat{d}(t)$ become larger. It can be ensured that the system can still converge with a smaller region. Owing to the fact that the control rate is nonsingular and continuous and there is no switching term in the general control rate, the chattering caused by frequent switching is avoided, so that the proposed control rate $u$ can get lower chattering.

## 4. Simulations

In order to verify the feasibility and effectiveness of the control method in this paper, the controlled object is taken as a single-stage inverted pendulum system, and its dynamic equation is

$$\begin{aligned} \dot{x}_1 &= x_2 \\ \dot{x}_2 &= f(\boldsymbol{x}) + b(\boldsymbol{x})\, u \end{aligned} \tag{50}$$

where $f(\boldsymbol{x}) = (g \sin x_1 - mlx_2^2 \cos x_1 \sin x_1/(m_c+m_p))/l(4/3 - m_p\cos^2 x_1/(m_c+m_p))$, $b(\boldsymbol{x}) = (\cos x_1/(m_c+m_p))/l(4/3 - m_p\cos^2 x_1/(m_c+m_p))$. $x_1$ and $x_2$ are, respectively, the swing angle and the swing speed, $u$ is the control input, $m_c$ is the weight of the trolley, $m_p$ is the weight of the pendulum, $l$ is the length of the pendulum, and $g$ is the acceleration of gravity.

The performance of system (50) contorted by the proposed method is compared with the NTSM control method [18] and the NFTSM control method [27] which are based on the following exponential reaching law.

(1) The sliding mode, the reaching law, and the controller of the NTSM control method based on the exponential reaching law are as follows:

$$\begin{aligned} s &= e_1 + \frac{1}{\beta} e_2^{q/p}, \\ \dot{s} &= -ws - \rho \operatorname{sgn}(s), \\ u &= -b(x)^{-1}\left[f(x) + \beta\frac{p}{q} e_2^{2-q/p} + ws + \rho \operatorname{sgn}(s) - \ddot{x}_d\right] \end{aligned} \tag{51}$$

(2) The sliding mode, the reaching law, and the controller of the NFTSM control method based on the exponential reaching law are as follows:

$$\begin{aligned} s &= e_1 + \alpha_1 |e_1|^{\gamma} \operatorname{sgn}(e_1) + \alpha_2 |e_2|^{q/p} \operatorname{sgn}(e_2), \\ \dot{s} &= -ws - \rho \operatorname{sgn}(s), \end{aligned}$$

Table 1: System model parameters.

| the weight of the trolley ($m_c$) | the weight of the pendulum ($m_p$) | the length of the pendulum ($l$) | the acceleration of gravity ($g$) |
|---|---|---|---|
| 1kg | 0.1kg | 0.5m | 9.8 $m/s^2$ |

Table 2: Controller parameters.

| parameter | NTSM | NFTSM | SPNFTSM | RBFSPNFTSM | RBFDOSPNFTSM |
|---|---|---|---|---|---|
| $\alpha_1$ | - | 0.1 | 0.1 | 0.1 | 0.1 |
| $\alpha_2$ | - | 0.02 | 0.02 | 0.02 | 0.02 |
| $\gamma$ | - | 27/19 | 27/19 | 27/19 | 27/19 |
| $\frac{q}{p}$ | 21/19 | 21/19 | 21/19 | 21/19 | 21/19 |
| $\beta$ | 10 | - | - | - | - |
| $w$ | 1000 | 1000 | - | - | - |
| $\rho$ | 1 | 1 | - | - | - |
| $k_3$ | - | - | 100 | 100 | 100 |
| $k_4$ | - | - | 1 | 1 | 0.1 |
| $c_2$ | - | - | 0.5 | 0.5 | 0.5 |
| $c_3$ | - | - | 1.5 | 1.5 | 1.5 |
| $k$ | - | - | - | - | 0.291 |

$$u = -b(\boldsymbol{x})^{-1}\left[f(\boldsymbol{x}) + \frac{1}{\alpha_2}\frac{p}{q}|e_2|^{2-q/p}\operatorname{sgn}(e_2)\left(1+\alpha_1\gamma|e_1|^{\gamma-1}\right) + ws + \rho\operatorname{sgn}(s) - \ddot{x}_d\right] \tag{52}$$

(3) The sliding mode, the reaching law, and the controller of the NFTSM control method based on the second power reaching law (SPNFTSM) are as follows:

$$\begin{aligned} s &= e_1 + \alpha_1|e_1|^{\gamma}\operatorname{sgn}(e_1) + \alpha_2|e_2|^{q/p}\operatorname{sgn}(e_2),\\ \dot{s} &= -k_3|s|^{c_2}\operatorname{sgn}(s) - k_4|s|^{c_3}\operatorname{sgn}(s),\\ u &= -b(\boldsymbol{x})^{-1}\left[f(\boldsymbol{x}) + \frac{1}{\alpha_2}\frac{p}{q}|e_2|^{2-q/p}\operatorname{sgn}(e_2)\left(1+\alpha_1\gamma|e_1|^{\gamma-1}\right) + k_3|s|^{c_2}\operatorname{sgn}(s) + k_4|s|^{c_3}\operatorname{sgn}(s) - \ddot{x}_d\right] \end{aligned} \tag{53}$$

(4) The sliding mode, the reaching law, and the controller of the NFTSM control method based on the second power of RBF network (RBFSPNFTSM) are as follows:

$$\begin{aligned} s &= e_1 + \alpha_1|e_1|^{\gamma}\operatorname{sgn}(e_1) + \alpha_2|e_2|^{q/p}\operatorname{sgn}(e_2),\\ \dot{s} &= -k_3|s|^{c_2}\operatorname{sgn}(s) - k_4|s|^{c_3}\operatorname{sgn}(s),\\ u &= -\widehat{b}(\boldsymbol{x})^{-1}\left[\widehat{f}(\boldsymbol{x}) + \frac{1}{\alpha_2}\frac{p}{q}|e_2|^{2-q/p}\operatorname{sgn}(e_2)\left(1+\alpha_1\gamma|e_1|^{\gamma-1}\right) + k_3|s|^{c_2}\operatorname{sgn}(s) + k_4|s|^{c_3}\operatorname{sgn}(s) - \ddot{x}_d\right] \end{aligned} \tag{54}$$

(5) The sliding mode, the reaching law, and the controller of the NFTSM control method based on the second power of RBF network and disturbance observer (RBFDOSPNFTSM) are as follows:

$$\begin{aligned} s &= e_1 + \alpha_1|e_1|^{\gamma}\operatorname{sgn}(e_1) + \alpha_2|e_2|^{q/p}\operatorname{sgn}(e_2),\\ \dot{s} &= -k_3|s|^{c_2}\operatorname{sgn}(s) - k_4|s|^{c_3}\operatorname{sgn}(s),\\ u &= -\widehat{b}(\boldsymbol{x})^{-1}\left[\widehat{f}(\boldsymbol{x}) + k\widehat{d}(t) + \frac{1}{\alpha_2}\frac{p}{q}|e_2|^{2-q/p}\operatorname{sgn}(e_2)\left(1+\alpha_1\gamma|e_1|^{\gamma-1}\right) + k_3|s|^{c_2}\operatorname{sgn}(s) + k_4|s|^{c_3}\operatorname{sgn}(s) - \ddot{x}_d\right] \end{aligned} \tag{55}$$

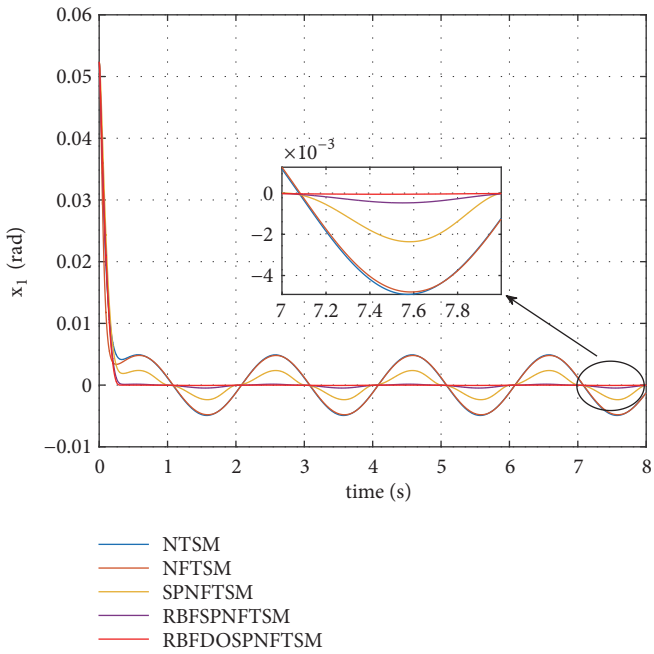


Figure 3: Swing angle response curve.

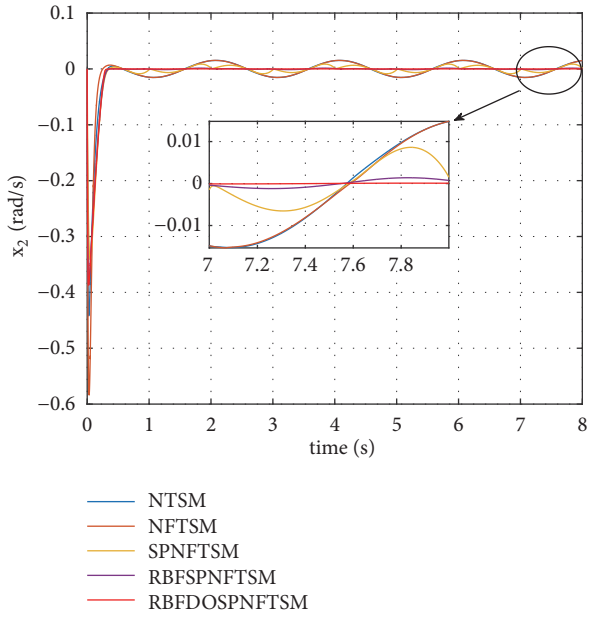


Figure 4: Swing speed response curve.

*4.1. Dynamic Performance Analysis.* The initial state of the inverted pendulum system is set as $[\pi/60, 0]$, and the system model parameters and controller parameters are shown in Tables 1 and 2, respectively. Given signal $x_d = 0$, interference $d(t) = \sin(x_1) + 5\sin(\pi t)$.

In order to better analyse the stability of the system, the following two performance evaluation indicators are adopted:

Table 3: Performance index values of the inverted pendulum system.

| | ISE | IAE |
|---|---|---|
| | $e_1$ | $e_1$ |
| NTSM | 2.0317e-04 | 0.0229 |
| NFTSM | 1.6484e-04 | 0.0211 |
| SPNFTSM | 2.0334e-04 | 0.0154 |
| RBFSPNFTSM | 1.5577e-04 | 0.0062 |
| RBFDOSPNFTSM | 1.5375e-04 | 0.0050 |

*(1) Integral of Error Squared Value (ISE)*

$$\mathrm{ISE} = \int_0^t x_i^{\,2}(\tau)\, d\tau \tag{56}$$

*(2) Integral of Absolute Value of Error (IAE)*

$$\mathrm{IAE} = \int_0^t \left| x_i(\tau) \right| d\tau \tag{57}$$

The performance index values of the inverted pendulum system for the above two evaluation methods are shown in Table 3. It can be seen from Table 3 that the performance evaluation index value of the state error $e_1$ of the control method used in this paper is smaller than other control methods. Therefore, the system stability of RBFDOSPNFTSM is better than that of other control methods.

Figures 3–6 show the response curves of the pendulum, swing speed, sliding mode, and system phase trajectory, respectively. It can be seen from them that the system state $x_1$, $x_2$ can converge to the equilibrium point at a faster speed

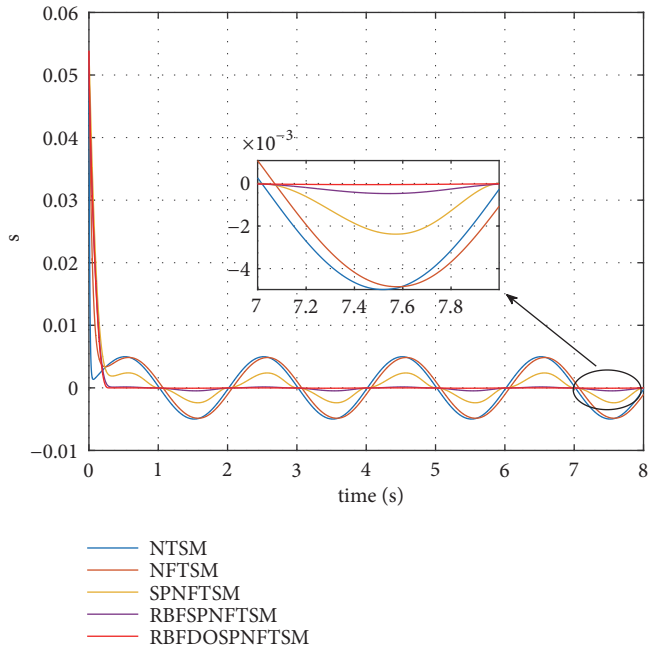


Figure 5: Sliding mode $s$ response curve.

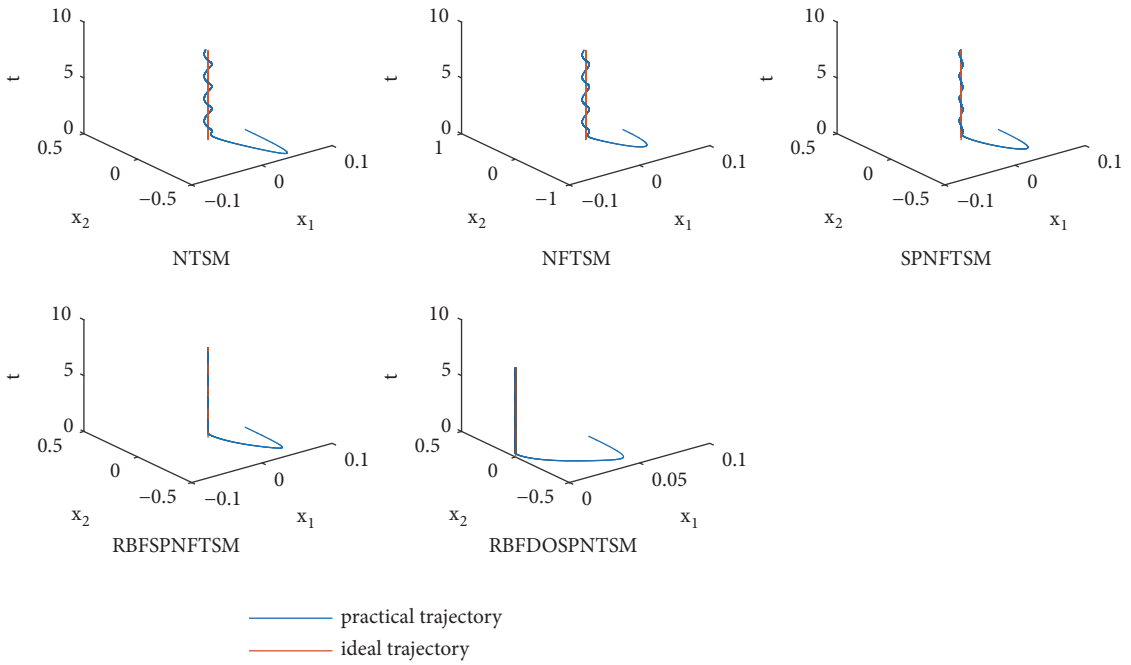


Figure 6: System phase trajectory three-dimensional curve.

under the control of the proposed scheme and can maintain a good stability state accuracy even if a large amount of interference is added. And the three-dimensional curve of the phase trajectory can intuitively show that the control process of the proposed method is smooth and jitter-free, and the system is more robust. Figure 7 shows the control input response curve. It can be seen from Figure 7 that the control method of the present invention controls the input signal to be smooth, which can reduce the wear of the motor. Figure 8 shows that the disturbance observer designed in this paper can estimate the interference value very well.

*4.2. Signal Tracking Analysis after Adding Noise.* If the initial states of the inverted pendulum system, system model

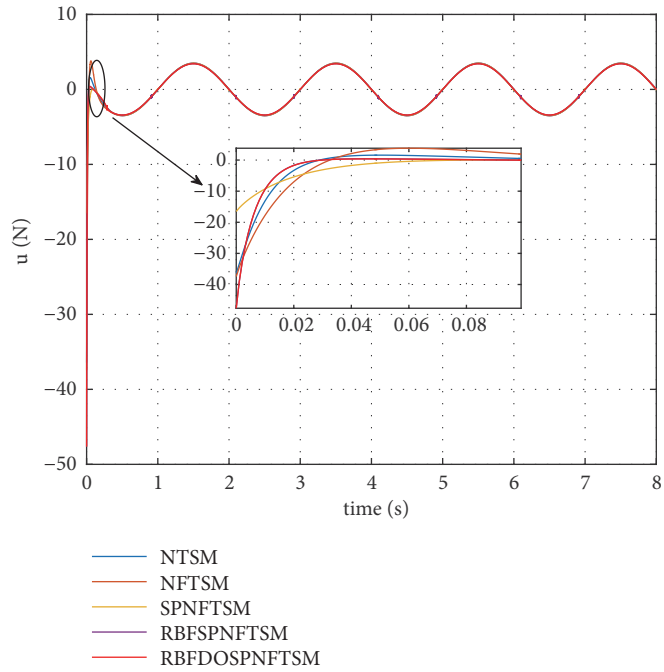


Figure 7: Control input response curve.

parameters, controller parameters, and interference remain unchanged, consider the given signal $x_d = x_{d1} + \eta n(t)$ with the noise signal to analyze the tracking control performance of the system, where $\eta = 0.0001$, $n(t)$ is a random number between [-1, 1], and $x_{d1}$ is shown as below:

$$x_{d1} = \begin{cases} 0.5t - \dfrac{1}{4\pi}\sin(2\pi t), & 0 \le t < 1 \\ 0.5, & 1 \le t < 2 \\ -0.5t + 1.5 + \dfrac{1}{4\pi}\sin(2\pi t), & 2 \le t < 3 \\ 0, & 3 \le t < 4 \\ -0.5t + 2 + \dfrac{1}{4\pi}\sin(2\pi t), & 4 \le t < 5 \\ -0.5, & 5 \le t < 6 \\ 0.5t - 3.5 - \dfrac{1}{4\pi}\sin(2\pi t), & 6 \le t < 7 \\ 0, & 7 \le t < 8 \end{cases} \tag{58}$$

Figures 9 and 10 show the swing angle tracking curve and the swing speed response curve of the inverted pendulum system with noise interference. It can be seen from Figures 9 and 10 that the control method of this paper has a poor suppression effect on noise and obvious chattering. Through the analysis of the control method of this paper, it is found that when the first and second derivatives are obtained for the given signal, a differential explosion phenomenon will be generated, and the noise signal in the given signal will be amplified. Therefore, the tracking differentiator needs to be designed to filter the given signal.

The augmented nonlinear tracking differentiator (ATD) proposed in [34] is used to filter the given signal and suppress the influence of the noise signal on the control system. Its expression is as follows:

$$\begin{aligned} \dot{z}_0(t) &= z_1(t) \\ \dot{z}_1(t) &= z_2(t) \\ \dot{z}_2(t) &= z_3(t) \\ \dot{z}_3(t) &= -R^4\left[sig\left(z_0(t) - \int v(\tau)\,d\tau; a_0, b\right) + sig\left(\frac{z_1(t)}{R}; a_1, b\right) + sig\left(\frac{z_2(t)}{R^2}; a_2, b\right) + sig\left(\frac{z_3(t)}{R^3}; a_3, b\right)\right] \\ sig(z; a_i, b) &= a_i\left[\left(1 + e^{-bz}\right)^{-1} - 0.5\right] \end{aligned} \tag{59}$$

where $a_0 > 0$, $a_1 > 0$, $a_2 > 0$, $a_3 > 0$, $b > 0$, $R > 0$, and $v(t)$ is an arbitrary bounded input signal. $z_1$, $z_2$, and $z_3$ are estimated values, estimated values of first-order derivative, and estimated values of second-order derivative of $v(t)$, respectively. Proof of stability has been given in [34]. The parameters of the augmented nonlinear tracking differentiator are shown in Table 4.

Table 4: Parameters of the augmented nonlinear tracking differentiator.

| $a_0$ | $a_1$ | $a_2$ | $a_3$ | $b$ | $R$ |
|---|---|---|---|---|---|
| 10 | 10 | 10 | 1 | 10 | 25 |

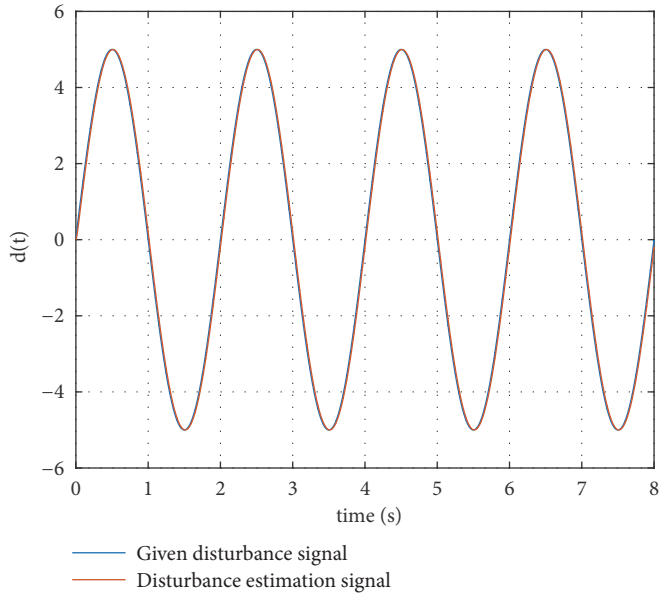


Figure 8: Disturbance observation result.

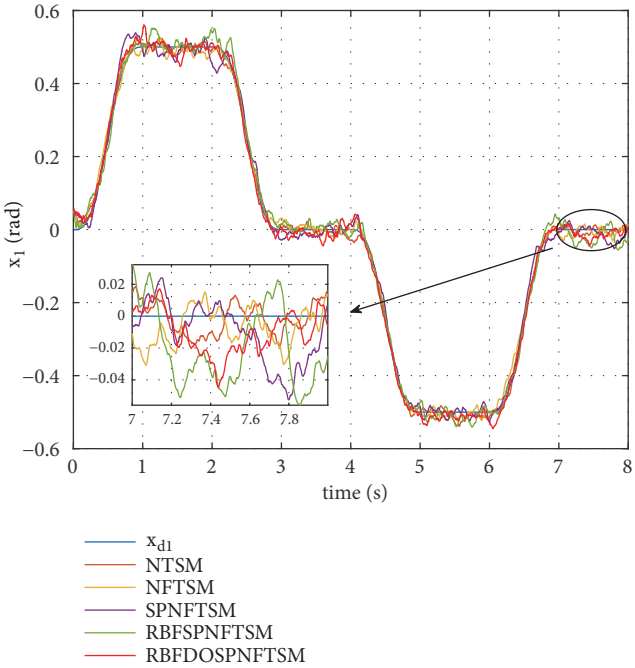


Figure 9: Swing angle tracking curve (adding noise).

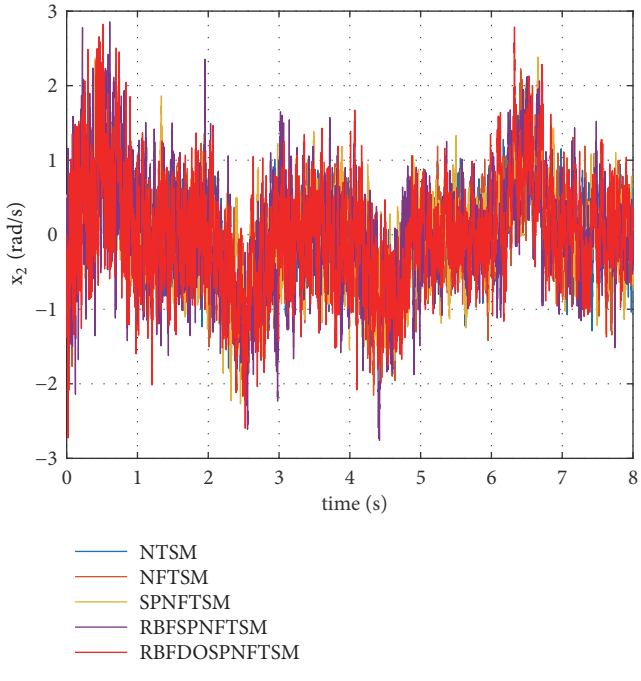


Figure 10: Swing speed response curve (adding noise).

Figures 11–14 are the response curves of the swing angle, swing speed, sliding mode, and system phase trajectory of the inverted pendulum system with noise interference and filtered by the tracking differentiator. It can be seen from Figures 11–14 that the RBFDOSPNFTSM control method for filtering of the given signal by the augmented nonlinear tracking differentiator (ATDRBFDOSPNFTSM) has advantages in tracking accuracy, suppression of chattering, and the dynamic quality. Figure 15 shows the control input response curve. It can be seen from Figure 15 that the control method adding the ATDRBFDOSPNFTSM has basically no chattering phenomenon and has advantages in actual energy consumption and mechanical wear of operation.

## 5. Conclusions

This paper proposes a nonsingular fast terminal sliding mode control scheme combining RBF network and disturbance observer to solve the tracking control problem of uncertain nonlinear systems. Firstly, the sliding mode controller is

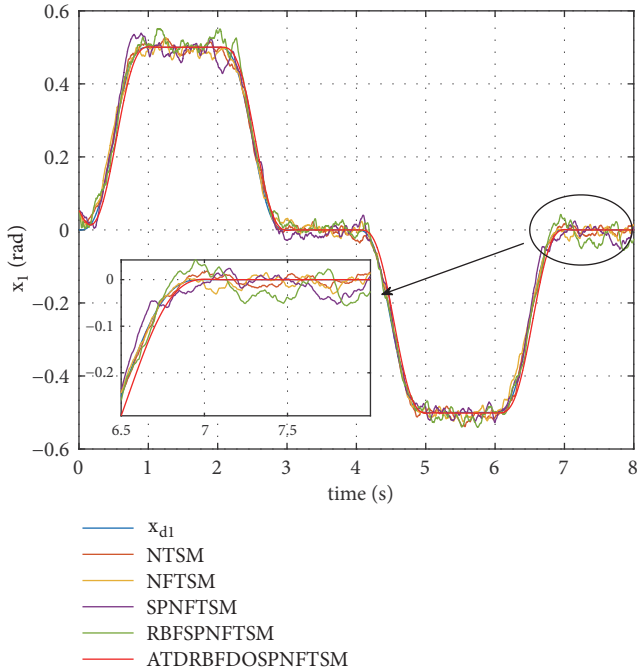


Figure 11: Swing angle tracking curve (adding noise).

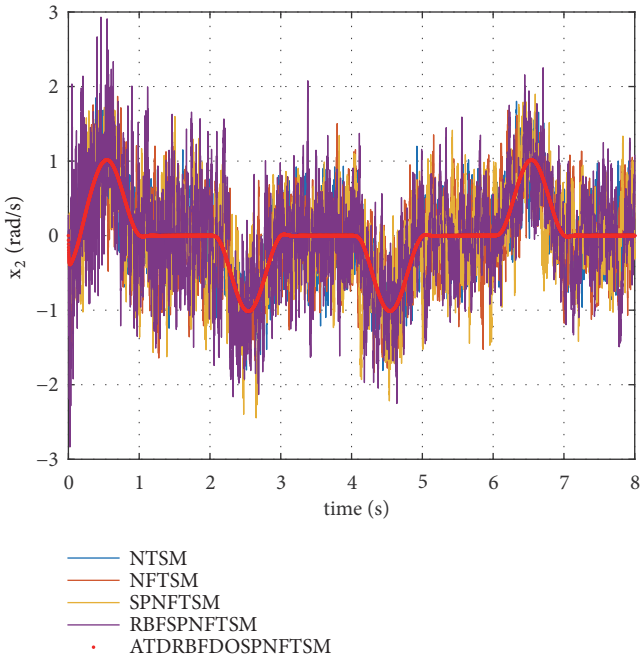


Figure 12: Swing speed response curve (adding noise).

designed by using nonsingular fast terminal sliding mode and second power reaching law to solve the problem of singularity and slow convergence of traditional terminal sliding mode control. Then, the unknown nonlinear function of the system is approximated by the RBF network, and the hyperbolic tangent disturbance observer is used to estimate the interference of the system and enhance the robustness of the system. Finally, the given signal is filtered by the augmented nonlinear tracking differentiator, eliminating the effects of noise in a given signal on the system. Through the numerical simulation results, the dynamic performance of the inverted pendulum system and the signal tracking of adding noise are analyzed. The control method can eliminate the noise pollution of a given signal, shorten the system arrival time, improve the tracking accuracy, and suppress the chattering phenomenon.

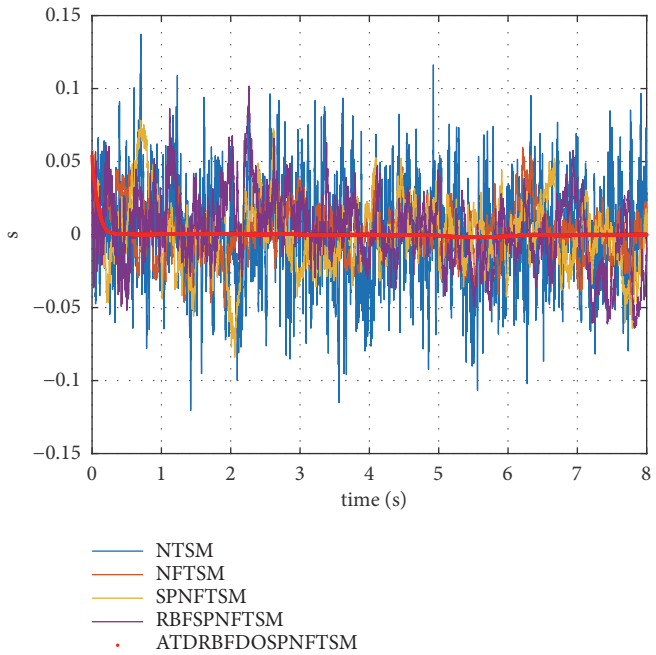


Figure 13: Sliding mode $s$ response curve (adding noise).

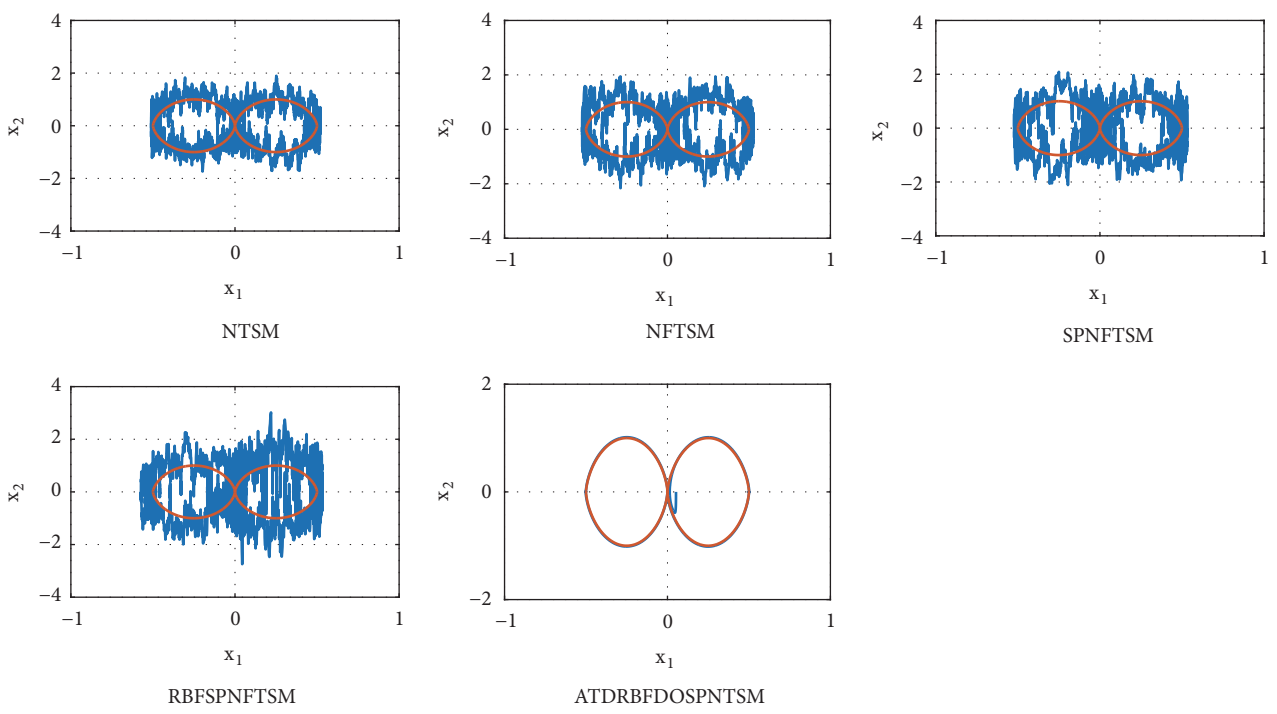


Figure 14: System phase trajectory curve (adding noise).

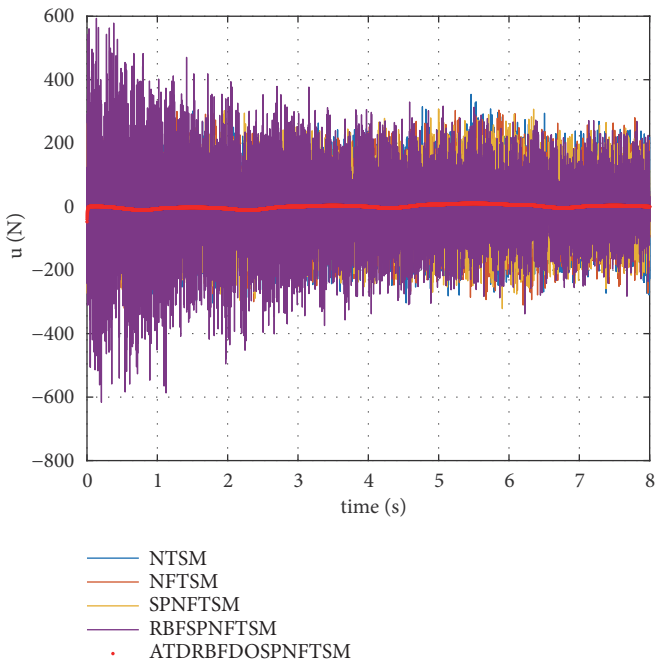


Figure 15: Control input response curve (adding noise).

## Data Availability

The data used to support the findings of this study are available from the corresponding author upon request.

## Conflicts of Interest

The authors declare that there are no conflicts of interest regarding the publication of this paper.

## References

[1] H. H. Choi, "Sliding-mode output feedback control design," *IEEE Transactions on Industrial Electronics*, vol. 55, no. 11, pp. 4047–4054, 2008.

[2] J. Liu, Y. Wu, J. Guo, and Q. Chen, "High-order sliding mode-based synchronous control of a novel stair-climbing wheelchair robot," *Journal of Control Science and Engineering*, vol. 2015, Article ID 680809, 16 pages, 2015.

[3] L. Yuan and H.-S. Wu, "Multiple-sliding-mode robust adaptive design for ship course tracking control," *Control Theory and Applications*, vol. 27, no. 12, pp. 1618–1622, 2010.

[4] M. L. Corradini and A. Cristofaro, "Nonsingular terminal sliding-mode control of nonlinear planar systems with global fixed-time stability guarantees," *Automatica*, vol. 95, pp. 561–565, 2018.

[5] B. Lu, Y. Fang, and N. Sun, "Continuous sliding mode control strategy for a class of nonlinear underactuated systems," *IEEE Transactions on Automatic Control*, vol. 63, no. 10, pp. 3471–3478, 2018.

[6] J. Fei and Z. Feng, "Adaptive fuzzy super-twisting sliding mode control for microgyroscope," *Complexity*, vol. 2019, Article ID 6942642, 13 pages, 2019.

[7] D. Qi, J. Feng, and J. Yang, "Longitudinal motion control of auv based on fuzzy sliding mode method," *Journal of Control Science and Engineering*, vol. 2016, Article ID 7428361, 7 pages, 2016.

[8] F. Baklouti, S. Aloui, and A. Chaari, "Adaptive fuzzy sliding mode tracking control of uncertain underactuated nonlinear systems: a comparative study," *Journal of Control Science and Engineering*, vol. 2016, Article ID 9283103, 12 pages, 2016.

[9] J. K. Liu and F. C. Sun, "Research and development on theory and algorithms of sliding mode control," *Control Theory & Applications*, vol. 24, no. 3, pp. 407–418, 2007.

[10] M. Zhihong and X. H. Yu, "Terminal sliding mode control of MIMO linear systems," *IEEE Transactions on Circuits and Systems I: Fundamental Theory and Applications*, vol. 44, no. 11, pp. 1065–1070, 1997.

[11] W. Gao, X. Chen, H. Du, and S. Bai, "Position tracking control for permanent magnet linear motor via continuous-time fast terminal sliding mode control," *Journal of Control Science and Engineering*, vol. 3, pp. 1–6, 2018.

[12] S. S. D. Xu, "Super-twisting-algorithm-based terminal sliding mode control for a bioreactor system," *Abstract and Applied Analysis*, vol. 2014, Article ID 495680, 9 pages, 2014.

[13] Y. Wu, X. Yu, and Z. Man, "Terminal sliding mode control design for uncertain dynamic systems," *Systems & Control Letters*, vol. 34, no. 5, pp. 281–287, 1998.

[14] Y. Tang, "Terminal sliding mode control for rigid robots," *Automatica*, vol. 34, no. 1, pp. 51–56, 1998.

[15] D. Y. Zhao, S. Y. Li, and F. Gao, "A new terminal sliding mode control for robotic manipulators," *International Journal of Control*, vol. 82, no. 10, pp. 1804–1813, 2009.

[16] X. Yu and M. Zhihong, "Multi-input uncertain linear systems with terminal sliding-mode control," *Automatica*, vol. 34, no. 3, pp. 389–392, 1998.

[17] W. Zhang and J. Wang, "Nonsingular terminal sliding mode control based on exponential reaching law," *Journal of Control and Decision*, vol. 27, no. 6, pp. 909–913, 2012.

[18] Y. Feng, X. Yu, and Z. Man, "Non-singular terminal sliding mode control of rigid manipulators," *Automatica*, vol. 38, no. 12, pp. 2159–2167, 2002.

[19] Y. Feng, S. Bao, and X. H. Yu, "Design method of non-singular terminal sliding mode control systems," *Journal of Control and Decision*, vol. 17, no. 2, pp. 194–198, 2002.

[20] S. B. Li, K. Q. Li, J. Q. Wang et al., "Nonsingular and fast terminal sliding mode control method," *Information and Control*, vol. 38, no. 1, pp. 1–8, 2009.

[21] J. H. Song, M. S. Song, and H. B. Zhou, "Adaptive nonsingular fast terminal sliding mode guidance law with impact angle constraints," *International Journal of Control, Automation, and Systems*, vol. 14, no. 1, pp. 99–114, 2016.

[22] J. W. Jeong, H. S. Yeon, and K.-B. Park, "Extended nonsingular terminal sliding surface for second-order nonlinear systems," *Abstract and Applied Analysis*, vol. 2014, Article ID 267510, 6 pages, 2014.

[23] M.-D. Tran and H.-J. Kang, "Nonsingular terminal sliding mode control of uncertain second-order nonlinear systems," *Mathematical Problems in Engineering*, vol. 2015, Article ID 181737, 8 pages, 2015.

[24] W. Wang, Q. Zhao, Y. Zhao, and D. Du, "A nonsingular terminal sliding mode approach using adaptive disturbance observer for finite-time trajectory tracking of mems triaxial vibratory gyroscope," *Mathematical Problems in Engineering*, vol. 2015, Article ID 205652, 8 pages, 2015.

[25] H. Wang, L. Shi, Z. Man et al., "Continuous fast nonsingular terminal sliding mode control of automotive electronic throttle systems using finite-time exact observer," *IEEE Transactions on Industrial Electronics*, vol. 65, no. 9, pp. 7160–7172, 2018.

[26] J. Yang, S. Li, J. Su, and X. Yu, "Continuous nonsingular terminal sliding mode control for systems with mismatched disturbances," *Automatica*, vol. 49, no. 7, pp. 2287–2291, 2013.

[27] S.-Y. Chen and F.-J. Lin, "Robust nonsingular terminal sliding-mode control for nonlinear magnetic bearing system," *IEEE Transactions on Control Systems Technology*, vol. 19, no. 3, pp. 636–643, 2011.

[28] L. Yang and J. Yang, "Nonsingular fast terminal sliding-mode control for nonlinear dynamical systems," *International Journal of Robust and Nonlinear Control*, vol. 21, no. 16, pp. 1865–1879, 2011.

[29] Y. Cheng and H. Lin, "Nonsingular fast terminal sliding mode positioning control in switched reluctance motor," *Electric Machines and Control*, vol. 16, no. 9, pp. 78–82, 2012.

[30] Z. He, C. Liu, Y. Zhan, H. Li, X. Huang, and Z. Zhang, "Nonsingular fast terminal sliding mode control with extended state observer and tracking differentiator for uncertain nonlinear systems," *Mathematical Problems in Engineering*, vol. 2014, Article ID 639707, 16 pages, 2014.

[31] C.-C. Hua, K. Wang, J.-N. Chen, and X. You, "Tracking differentiator and extended state observer-based nonsingular fast terminal sliding mode attitude control for a quadrotor," *Nonlinear Dynamics*, vol. 94, no. 1, pp. 343–354, 2018.

[32] A. Mohammadi, M. Tavakoli, H. J. Marquez, and F. Hashemzadeh, "Nonlinear disturbance observer design for robotic manipulators," *Control Engineering Practice*, vol. 21, no. 3, pp. 253–267, 2013.

[33] J. Huang, S. Ri, L. Liu, Y. Wang, J. Kim, and G. Pak, "Nonlinear disturbance observer-based dynamic surface control of mobile wheeled inverted pendulum," *IEEE Transactions on Control Systems Technology*, vol. 23, no. 6, pp. 2400–2407, 2015.

[34] X. W. Bu, X. Y. Wu, Y. X. Chen et al., "Design of a class of new nonlinear disturbance observers based on tracking differentiators for uncertain dynamic systems," *International Journal of Control Automation & Systems*, vol. 13, no. 3, pp. 595–602, 2015.

[35] X. Shao, J. Liu, J. Li, H. Cao, C. Shen, and X. Zhang, "Augmented nonlinear differentiator design and application to nonlinear uncertain systems," *ISA Transactions*, vol. 67, pp. 30–46, 2017.

[36] G. Marks, Y. Shtessel, H. Gratt, and I. Shkolnikov, "Effects of high order sliding mode guidance and observers on hit-to-kill interceptions," in *Proceedings of the AIAA Guidance, Navigation, and Control Conference and Exhibit*, American Institute of Aeronautics and Astronautics, San Francisco, Calif, USA, 2005.

[37] M. Haijie, L. Wei, and F. Xiaolin, "Nonlinear tracking differentiator design based on hyperbolic tangent," *Computer Applications*, vol. 36, no. s1, pp. 305–309, 2016.